Developmental Biology 462 (2020) 208–222

Contents lists available at ScienceDirect

Developmental Biology

journal homepage: www.elsevier.com/locate/developmentalbiology

A PI4KIIIα protein complex is required for cell viability during *Drosophila* wing development

Urbashi Basu, Sruthi S. Balakrishnan, Vishnu Janardan, Padinjat Raghu *

National Centre for Biological Sciences-TIFR, GKVK Campus, Bellary Road, Bangalore, 560065, India

ARTICLE INFO

Keywords:
Wing development
Plasma membrane
Cell death
Imaginal discs
Drosophila
Phosphoinositides
Signalling

ABSTRACT

Phosphatidylinositol 4 phosphate (PI4P) and phosphatidylinositol 4,5 bisphosphate [PI(4,5)P_2] are enriched on the inner leaflet of the plasma membrane and proposed to be key determinants of its function. PI4P is also the biochemical precursor for the synthesis of PI(4,5)P_2 but can itself also bind to and regulate protein function. However, the independent function of PI4P at the plasma membrane in supporting cell function in metazoans during development *in vivo* remains unclear. We find that conserved components of a multi-protein complex composed of phosphatidylinositol 4-kinase IIIα (PI4KIIIα), TTC7 and Efr3 is required for normal vein patterning and wing development. Depletion of each of these three components of the PI4KIIIα complex in developing wing cells results in altered wing morphology. These effects are associated with an increase in apoptosis and can be rescued by expression of an inhibitor of *Drosophila* caspase. We find that in contrast to previous reports, PI4KIIIα depletion does not alter key outputs of hedgehog signalling in developing wing discs. Depletion of PI4KIIIα results in reduced PI4P levels at the plasma membrane of developing wing disc cells while levels of PI(4,5)P_2, the downstream metabolite of PI4P, are not altered. Thus, PI4P itself generated by the activity of the PI4KIIIα complex plays an essential role in supporting cell viability in the developing *Drosophila* wing disc.

1. Introduction

The phosphorylation of the lipid phosphatidylinositol (PI) in a position specific manner generates signalling molecules that tune ongoing cellular and physiological processes in animal cells (Balla, 2013). Positions 3, 4, 5 of the inositol headgroup can be phosphorylated combinatorically to generate 7 molecules; 3 monophosphates, 3 bisphosphates and one trisphosphate. Of these, phosphatidylinositol 4,5 bisphosphate [PI(4,5)P_2] and the precursor from which it is synthesized, phosphatidylinositol 4 phosphate (PI4P) are the most abundant in cells. PI (4,5)P_2 is primarily distributed at the plasma membrane where it supports a number of key cellular functions [reviewed in Kolay et al. (2016)]. PI4P is synthesized by phosphatidylinositol 4-kinases (PI4K), enzymes that can phosphorylate phosphatidylinositol at position 4; multiple genes that encode distinct PI4K enzyme isoforms with unique properties have been identified that are proposed to generate distinct pools of PI4P at organelle membranes. For example, in the model eukaryote *Saccharomyces cerevisiae*, the gene *pik1* encodes a PI4K isoform that localizes to and generates PI4P at the Golgi (Walch-Solimena and Novick, 1999), whereas *stt4* encodes a PI4K that generates PI4P at the plasma membrane (Audhya and Emr, 2002). In metazoan models too, a number of distinct isoforms of PI4K are present (Altan-Bonnet and Balla, 2012). In *Drosophila* for example, *fwd* which encodes for PI4KIIIβ activity has been linked to Rab11 localization and spermatid viability (Brill et al., 2000; Giansanti et al., 2007; Polevoy et al., 2009). Recently, cell biological studies have identified PI4KIIIα, the ortholog of *stt4,* as the PI4K isoform that localizes to and generates PI4P at the plasma membrane (Nakatsu et al., 2012). Null mutants in PI4KIIIα are organismal lethal in mouse (Nakatsu et al., 2012) and cell and organismal lethal in *Drosophila* (Tan et al., 2014; Yan et al., 2011). However, tissue-specific RNAi mediated depletion of *Drosophila* PI4KIIIα (*dPI4KIIIα*) has recently shown that in *Drosophila* photoreceptors, PI4KIIIα activity is required to support the levels of PI4P and PI(4,5)P_2 at the plasma membrane during G-protein coupled PLC activation (Balakrishnan et al., 2018; Liu et al., 2018).

PI(4,5)P_2 and PI4P have both been implicated in regulating growth, development and patterning tissues in metazoans. Embryonic development in mammals is triggered by PI(4,5)P_2 hydrolysis and consequent Ca^{2+} influx to activate the egg (Swann and Lai, 2016). In *Drosophila*, PI(4,5)P_2 hydrolysis is necessary for cytokinesis in developing spermatids and for maintaining flagellar structure and ciliary transition zone in these cells (Gupta et al., 2018; Tan and Brill, 2014; Wei et al., 2003; Wong et al., 2005). PI4P metabolism itself is implicated in development;

* Corresponding author.
E-mail address: praghu@ncbs.res.in (P. Raghu).

https://doi.org/10.1016/j.ydbio.2020.03.008
Received 31 October 2019; Received in revised form 6 March 2020; Accepted 7 March 2020
Available online 17 March 2020

mutants of SacI, a lipid phosphatase that degrades PI4P shows defective dorsal closure in *Drosophila* (Wei et al., 2003). PI4KIIIα has also been linked to developmental processes; depletion of *dPI4KIIIα* in the ovary affects cortical actin organization, endocytosis, cell polarity and cell viability (Tan et al., 2014; Yan et al., 2011) and in *Drosophila* neural development, *dPI4KIIIα* is required for asymmetric division of neural stem cells (Koe et al., 2018). However, these processes are also known to depend on PI(4,5)P_2 levels and cellular mechanisms that depend on PI4P itself remain to be identified.

In the course of development, morphogen signalling is used to define local cell shape and size and sculpt tissue architecture (Dekanty and Milán, 2011). The patterning of the *Drosophila* wing during development has been extensively used as a model to study morphogen signalling. The wing imaginal disc is patterned by developmental cues that generate a specific arrangement of veins in the adult wing and stereotypic phenotypes are reported for defects in signalling pathways controlling this process. Phosphoinositides have been implicated in this process; for example, modulation of Type II PI3K (an enzyme that generates phosphatidylinositol 3 phosphate) impacts patterning in the wing in the context of EGF and Notch signalling (MacDougall et al., 2004). Signalling by the morphogen Hedgehog *(hh*) is also known to impact wing development (Briscoe and Thérond, 2013). A study in *Drosophila* wing discs has implicated PI4P metabolism in regulating *hh* signalling (Yavari et al., 2010) and electrostatic interactions between the polar head group of PI4P and arginine rich clusters at the c-terminus of Smo, a plasma membrane component of the *hh* signalling pathway are reported (Jiang et al., 2016). While these studies suggest a role for PI4P metabolism in *hh* signalling, the consequence of altered plasma membrane PI4P levels on patterning and development in the adult wing remains unknown. In a genetic screen for novel functions of phosphoinositide signalling, we identified a role for a multi-protein complex that is required to regulate plasma membrane PI4P levels and generate the normal vein pattern to generate the normal shape of the adult *Drosophila* wing. This complex is made up of three proteins, dPI4KIIIα, dTTC7 and StmA. In cells of the developing wing disc, depletion of this complex results in reduced levels of plasma membrane PI4P but is not associated with concomittant changes in levels of PI(4,5)P_2. Surprisingly, we found that depletion of the dPI4KIIIα complex does not alter *hh* signalling in the developing wing disc. Rather, we found that depletion of this complex in the developing wing results in enhanced cell death. Thus, the activity of the dPI4KIIIα complex is required to support cell viability but not *hh* signalling during the tissue patterning events during *Drosophila* wing development.

2. Results

2.1. Depletion of dPI4KIIIα during development impacts patterning of the adult wing

We studied the consequence of reduced *dPI4KIIIα* function on wing patterning by depleting this gene using RNAi (*dPI4KIIIα*^{i}) in selected compartments of the developing wing. The part of the larval wing disc in which the manipulations were carried out and the corresponding part of the adult tissue are depicted schematically in supplementary Fig 1A. When *dPI4KIIIα*^{i} was expressed in cells of the developing anterior compartment (*ci* > *dPI4KIIIα*^{i}) at 18 °C, there was considerable lethality and very few adult flies of the desired genotype eclosed. The limited number of *ci* > *dPI4KIIIα*^{i} flies that did emerge showed a reduction in the size of the anterior compartment of the adult wing (Fig. 1Ai vs Aii). The observed wing defect and associated lethality could both be rescued by reconstituting human PI4KIIIα in the *dPI4KIIIα* depletion background (Fig. 1Ai vs Aiii) and ectopic expression of the hPI4KIIIα transgene by itself in the same wing domain did not result in a wing defect (Fig. 1Ai vs Aiv). Likewise, when *dPI4KIIIα* was downregulated in the posterior compartment (*hh* > *dPI4KIIIα*^{i}), once again this resulted in partial lethality with lower than expected numbers of enclosing progeny. In those flies that eclosed, the size of the posterior compartment was reduced (Fig. 1Bi vs Bii). Additionally, in *hh* > *dPI4KIIIα*^{i} flies, the entire wing was curled, probably due to the different sizes of the anterior and posterior compartment. The defective wing due to depletion of *dPI4KIIIα* was completely rescued by expression of hPI4KIIIα in the (Fig. 1Bi vs Biii). No wing defects resulted due to ectopic expression of the human transgene in the *hh* domain (Fig. 1Bi vs Biv). In *ap* > *dPI4KIIIα*^{i}, where the RNAi was expressed in the dorsal compartment of the wing disc, complete lethality was observed even at 18 °C precluding an analysis of adult vein pattern.

In order to characterize the wing patterning defect, *dPI4KIIIα* depletion was carried out along the antero-posterior compartment boundary (*ptc* > *dPI4KIIIα*^{i}), since there was minimum lethality associated with this driver at 18 °C. In adult flies of *ptc* > *dPI4KIIIα*^{i}, we noted the loss or extra cuticle deposition in and around the anterior cross vein (ACV) (Fig. 1Ci vs Cii) as well a reduction of the distance between the L3-L4 longitudinal veins of the wings (quantified in Fig. 1 D). This observation was seen with more than one independent RNAi line designed against *dPI4KIIIα* (see supplementary Fig1Bi vsBii and Biii). The venation patterning defect observed with *ptc* > *dPI4KIIIIα*^{i} could be rescued by reconstituting hPI4KIIIα in *ptc* domain cells (*ptc* > *dPI4KIIIα*^{i}; *hPI4KIIIα*) (Fig. 1Ci, iii) whereas ectopic expression of the human transgene in *ptc* domain cells resulted in only a small increase in L3-L4 inter-vein distance with no other patterning defects (Fig. 1C iv).

2.2. dPI4KIIIα regulates PI4P levels at plasma membrane

To test if the phenotypes resulting from *dPI4KIIIα* knockdown were a consequence of reduced plasma membrane PI4P levels, we generated transgenic flies expressing a GFP tagged probe that has been used for quantifying changes in PI4P levels at the plasma membrane (P4M::GFP) in mammalian cells and *Drosophila* photoreceptors (Hammond et al., 2014; Balakrishnan et al., 2018). When expressed in *Drosophila* S2R + cells, P4M::GFP localized to the plasma membrane along with some punctate distribution within the cell (Fig. 2Ai vs iii). The expression of the probe was verified by a western blot using an anti-GFP antibody (Fig. 2B). Using the P4M::GFP probe in the third instar wing discs of *ptc* > *dPI4KIIIα*^{i} reared at 25 °C, we quantified plasma membrane PI4P levels; the ratio of plasma membrane/cytosolic P4M::GFP fluorescence reports the level of PI4P at the plasma membrane as compared to the underlying cytoplasm. We found that plasma membrane PI4P as measured using the P4M::GFP probe was reduced in *ptc* > *dPI4KIIIα*^{i} when compared to controls (Fig. 2Ci, ii and graph D). These measurements suggest that PI4P levels at the plasma membrane are lower when *dPI4KIIIα* is depleted. Expression of the P4M::GFP probe alone in otherwise wild type cells (Fig. 2Ei) did not result in any venation defect and expression of P4M::GFP in *ptc* > *dPI4KIIIα*^{i} showed no further alteration of the wing patterning defect of *ptc* > *dPI4KIIIα*^{i} (Fig. 2Eii, iii). Thus, the P4M probe itself did not impact PI4P dependent processes when expressed in developing *Drosophila* cells under our experimental conditions.

2.3. Wing defects in ptc > dPI4KIIIα^{i} are distinct from those with reduced PI(4,5)P_2 levels

In eukaryotic cells, a principal function of PI4P is to serve as substrate for the synthesis of the key plasma membrane lipid PI(4,5)P_2. In developing *Drosophila* oocytes, loss of *dPI4KIIIα* is reported to phenocopy PI(4,5)P_2 depletion (Tan et al., 2014). We tested if the phenotypes arising from *ptc* > *dPI4KIIIα*^{i} were a consequence of lower PI(4,5)P_2 due to the reduced availability of PI4P for its synthesis. The *Drosophila* genome contains two genes, *sktl* and *dPIP5K* that encode phosphatidylinositol 4 phosphate 5-kinase, the enzyme that converts PI4P into PI(4,5)P_2 (Balakrishnan et al., 2015). Using qRT-PCR of wild type 3rd instar wing discs, we were able to detect the expression of only *sktl* in this tissue at this developmental stage (Fig. 3A). We down regulated *sktl* function using two approaches: expression of a kinase dead dominant negative construct (*ptc* > *sktl*$^{K/D}$*::RFP*) (Fig. 3Bi, ii, and graph C) and depletion of *sktl* transcript (*ptc*

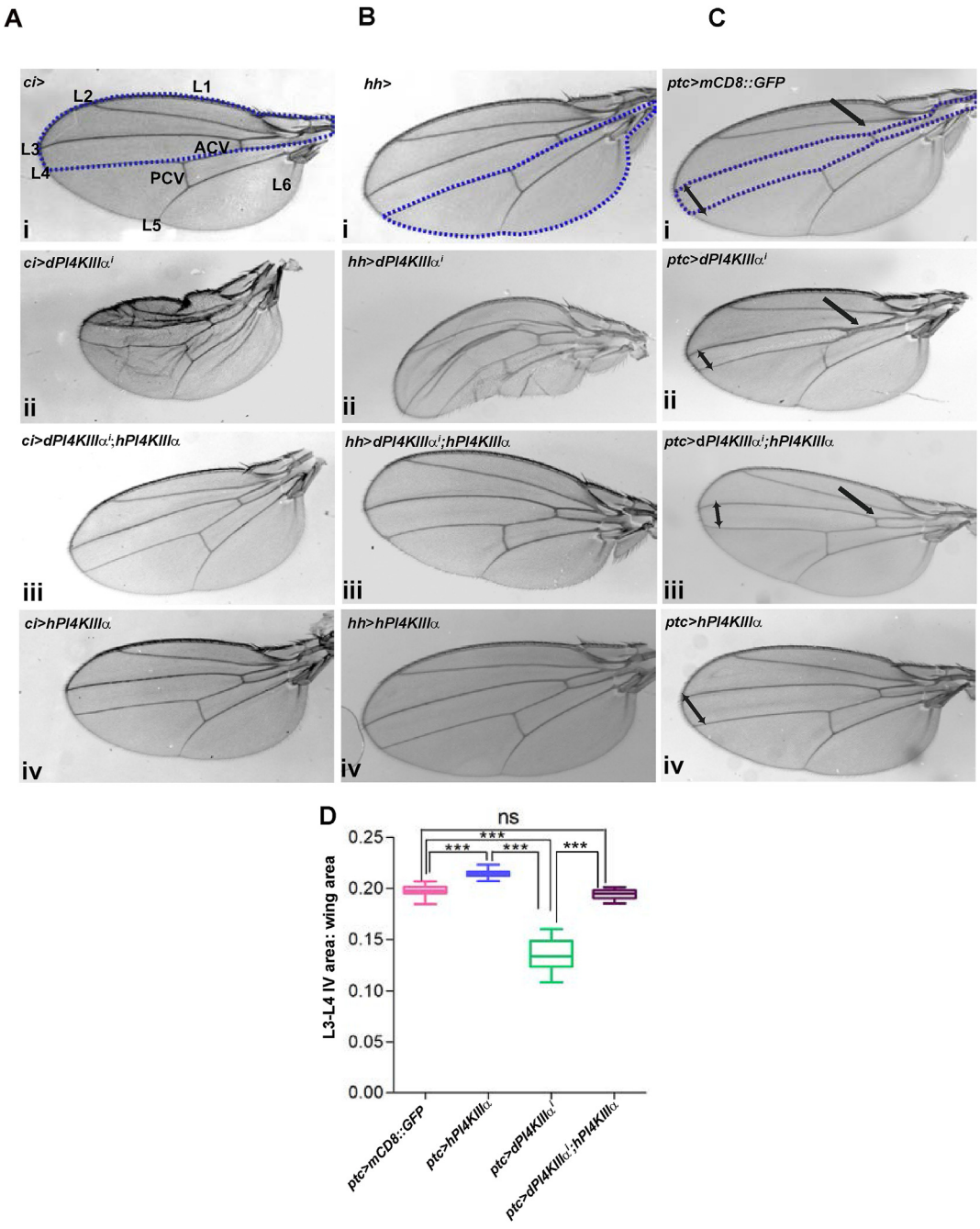

Fig. 1. Knockdown of *dPI4KIIIα* affects shape and venation patterning of adult wings.
Ai, Bi, Ci) Control wings of the indicated Gal4 drivers for anterior compartment (*ci*-Gal4), posterior compartment (*hh*-Gal4) and anterior cells close to A/P compartment boundary of (*ptc*-Gal4), respectively. L1-L6 are the longitudinal veins; ACV and PCV are anterior and posterior cross vein respectively. **Aii, Bii and Cii)** *ci* > *dPI4KIIIα*, *hh* > *dPI4KIIIα*^{i} and *ptc* > *dPI4KIIIα*^{i} wings. In case of Aii and Bii the respective compartment is shortened. In Cii (*ptc* > *dPI4KIIIα*^{i}) the inter-vein between L3 and L4 is shortened and the area around the ACV has disorganized extra cuticle deposition leading to a 'smudged' ACV. **Aiii, Biii, Ciii)** Rescue with the human PI4KIIIα transgene. **Aiv, Biv, Civ)** Ectopic expression of human PI4KIIIα in the respective domains of otherwise wild type discs. **D)** Quantification of the L3-L4 inter-vein distance of the wings represented in Cii, n ≥ 20 for each genotype for quantification. All experiments were repeated thrice and one set with corresponding data numbers (n) is reported here. For the current set, Aii n = 20, Bii n = 8, Cii n = 70. The region of genetic manipulation is demarcated by blue dotted lines. In case of C, the L3-L4 inter-vein distance shortening is pointed out with black arrow heads and the 'smudging' of ACV with black arrows.

> *sktl*^{i}) (Fig. 3Di, ii and graph E). Although both of these approaches resulted in a loss of the ACV in a large proportion of flies of the correct genotype (Fig. 3Bi, ii and Ci vs ii), they resulted in only a very modest reduction of the L3/L4 wing area (Fig. 3 graph F). This was in sharp contrast to *dPI4KIIIα* depletion that results in almost 40% reduction in the L3-L4 inter-vein distance. Lastly, we measured PI(4,5)P_2 levels at the plasma membrane of wing discs cells in *ptc* > *dPI4KIIIα*^{i} using the well-established PI(4,5)P_2 probe PH-PLCδ::mCherry and found no change in the levels of this lipid at the plasma membrane of *ptc* > *dPI4KIIIα*^{i} cells (Fig. 3Gi, ii and graph 3H). To test the effectiveness of *ptc* > *sktl*^{i} in reducing PI(4,5)P_2 levels, we attempted to measure the localization of PH-PLCδ::mCherry in *ptc* > *sktl*^{i} wing discs; these experiments showed a reduction in PI(4,5)P_2 levels (quantified in graph H). Together these findings strongly suggested that the vein patterning defects in *ptc* > *dPI4KIIIα*^{i} flies are unlikely to result from depletion of PI(4,5)P_2 consequent to a shortfall of plasma membrane PI4P.

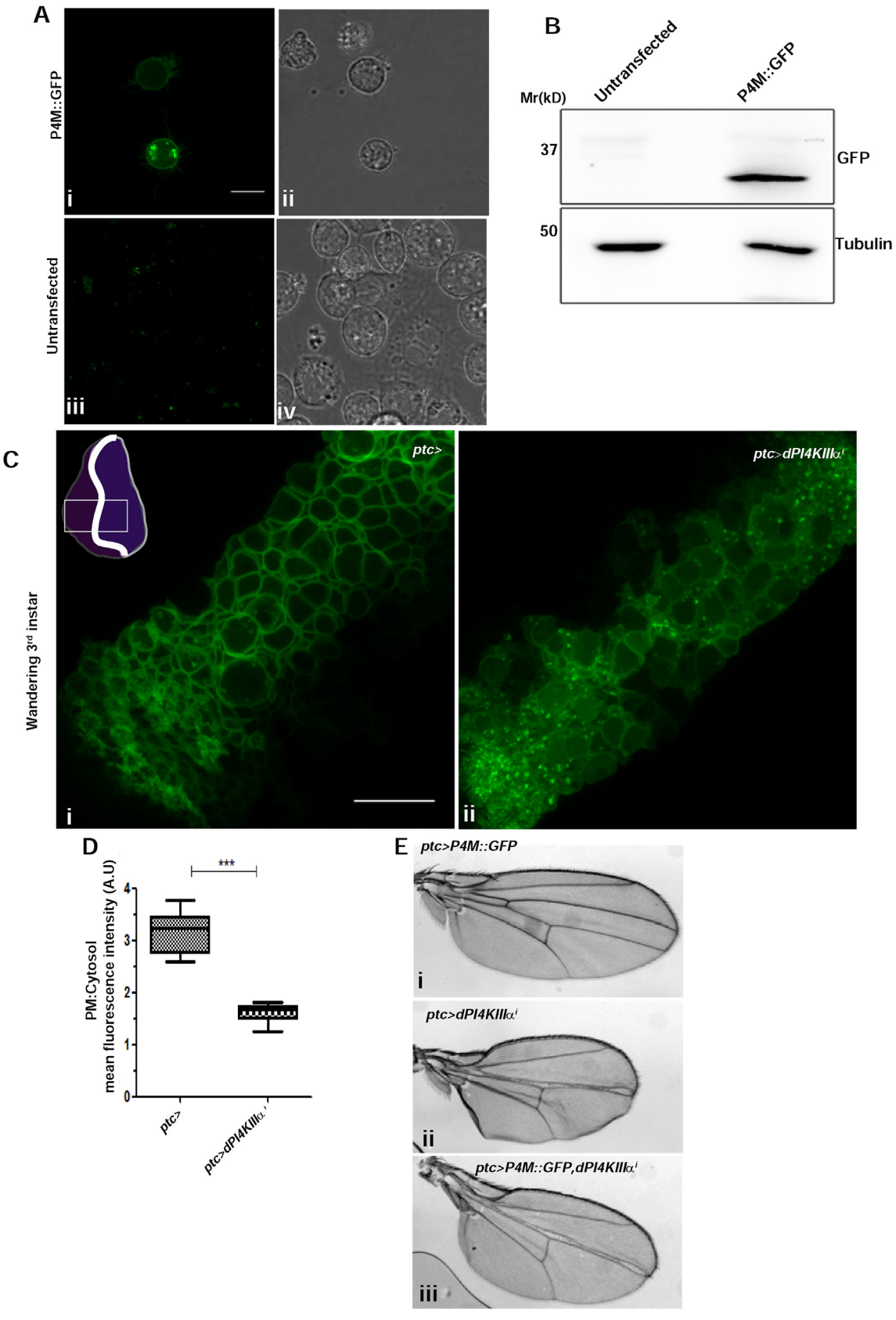

(caption on next page)

2.4. Down regulation of TTC7 and stmA phenocopies dPI4KIIIα depletion

In both yeast (Audhya and Emr, 2002) and mammalian cells (Nakatsu et al., 2012), PI4KIIIα is reported to function as part of a complex with the proteins TTC7 and Efr3. We recently identified and analysed the function of the *Drosophila* orthologs of TTC7 and EFR3 i.e. CG8325, *l(2)k14710* or dTTC7 and CG8739 (*stmA*) respectively (Balakrishnan et al., 2018). To test if these proteins were also required to pattern adult wing veins, we downregulated each of them individually in the *ptc* domain of otherwise wild type flies. *ptc* > *stmA*^{i} gave equivalent vein patterning defects (Fig. 4Ai and ii) to those seen in *ptc* > *dPI4KIIIα*^{i} and these defects could be partly rescued by reconstituting these cells with the mouse ortholog of *stmA*, mEFR3B (Nakatsu et al., 2012) (Fig. 4Aii and iii and graph C). Likewise, *ptc* > *dTTC7*^{i} resulted in a shortening of the L3-L4 inter-vein distance along with loss/smudging of the ACV (Fig. 4Bi vs ii). These defects were completely rescued by the expression of human TTC7*B* (Nakatsu et al., 2012) in *ptc* > *dTTC7*^{i} cells (Fig. 4B ii, iii and graph D). Downregulation of *dTTC7* and *stmA* using stronger GAL4 drivers expressing in other wing domains such as *ci*, *hh* and *ap*-Gal4 resulted in fully penetrant pupal lethality even at 18 °C, thus limiting venation patterning analysis. Measurement of PI4P levels using the P4M::GFP probe in the third instar wing discs of *ptc* > *stmA*^{i} and *ptc* > *dTTC7*^{i} reared at 25 °C showed a decrease in plasma membrane PI4P levels (Fig. 4Ei, ii and iii). The effect of knock down of *dTTC7* and *stmA* was so severe that the wing disc cells almost had no P4M probe localization at the plasma membrane; hence, it was difficult to quantify it. The finding that effects of *dTTC7* and *stmA* downregulation phenocopy those seen with *ptc* > *dPI4KIIIα*^{i} suggests that all three proteins affect similar sub-cellular processes in *ptc* domain cells during wing development. We also tested the effect of *ptc* > *dPI4KIIIα*^{i} along with simultaneous down regulation of either *dTTC7* or *stmA* in the same cells; this resulted in pupal lethality even at 18 °C.

2.5. Developmental timing of patterning defects seen by ptc > dPI4KIIIα^{i}

Since our data showed that *dPI4KIIIα* depletion affects normal wing development, we sought to determine the developmental time at which the venation defect of *ptc* > *PI4KIIIα*^{i} arises. The pattern of veins and inter-veins seen in the adult *Drosophila* wing is laid down as early as third instar larval stages (for the longitudinal veins) and further refined during pupal development. To understand the earliest time at which the L3-L4 inter-vein distance was altered due to *dPI4KIIIα* depletion, we studied the temporal course of these early events. To mark and follow the vein and inter-vein regions, we stained pupal wing discs at various developmental stages with an antibody to the protein Blistered that marks inter-vein cells [24] thereby distinguishing the pro-veins by negative staining. During the wandering 3rd instar larval stage no difference was observed in the pattern of Blistered staining between control and *ptc* > *dPI4KIIIα*^{i} discs (Fig. 5Ai', ii'); this was also the case when *dTTC7* (Fig. 5 Ai', iii') and *stmA (*Fig. 5Ai', iv') were depleted in the *ptc* domain. However, by 6 h APF *ptc* > *dPI4KIIIα*^{i} wings showed a reduction in the L3-L4 inter-vein distance (Fig. 5B i', ii' and graph C) as negatively outlined by Blistered staining. This phenotype was also clearly seen in case of *dTTC7* and *stmA* RNAi using *ptc-GAL4* (Fig. 5Bi', iii' and iv' and graph D and E respectively). Thus, the vein patterning defects seen *ptc* > *dPI4KIIIα*^{i} are established by 6 h APF at 25 °C.

2.6. Depletion of dPI4KIIIα does not affect cell division but causes apoptosis in the developing wing

In principle, two mechanisms can explain the reduced size of the wing domain where *dPI4KIIIα* is depleted. One possibility is a reduced number of cell divisions giving rise to fewer cells in the corresponding region of the developing wing. To test this, we carried out phospho-histone 3 (PH3) staining in third instar larval wing discs (Fig. 6A i' vs ii') and 6 h APF pupal wing discs (Fig. 6Bi' vs ii') to check for differences in cell division between control and *ptc* > *dPI4KIIIα*^{i}. PH3 staining was comparable between controls and *ptc* > *dPI4KIIIα*^{i} suggesting that defects in cell division do not underlie the reduced L3-L4 inter-vein area. In addition, when checked in *hh* > *dPI4KIIIα*^{i} (Fig. 6Ci vs ii) and *ci* > *dPI4KIIIα*^{i} (Fig. 6Di vs ii), there were no differences in cell divisions between control and *dPI4KIIIα* depleted wing discs in the respective wing domains. In addition, we also measured the mitotic index of *ci*>and *ci* > *dPI4KIIIα*^{i} wing discs (Fig. 6E) and found no difference between control and *pi4kIIIα* depleted discs.

An alternative possibility is that reduced dPI4KIIIα activity results in enhanced cell death and consequently a reduced L3-L4 inter-vein area. We used immunolabelling for *Drosophila* cleaved Caspase (Dcp-1) to detect ongoing apoptotic cell death. In control pupal wing discs at 6 h APF, there is minimal staining for Dcp-1; however, *ptc* > *dPI4KIIIα*^{i} discs at the same age showed enhanced Dcp-1 staining indicative of ongoing cell death (Fig. 7Ai' vs ii'). In case of the rescue genotype i.e., expression of *hPI4KIIIα* in *ptc* > *dPI4KIIIα*^{i}, Dcp-1 staining was reduced to that seen in control discs (see Fig. 7A ii' vs iii'). In *ptc* > *dTTC7*^{i} and *ptc* > *stmA*^{i} as well, increased cell death was detected by positive Dcp-1 staining (Fig. 7Bi' vs ii and iii'). Further, depletion of the *dPI4KIIIα* in the anterior (*ci*-GAL4) or posterior (*hh*-GAL4) compartments also caused increased cell death presumably resulting in changes in the shape of adult wing (Fig. 7Ci vs ii and Di vs ii respectively). Moreover, in wandering 3rd instar larvae where *ap*-GAL4 (expressed in the dorsal wing compartment encompassing anterior and posterior parts) was used to deplete *dPI4KIIIα, dTTC7* or *stmA,* enhanced Dcp-1 staining was observed in each case (7E i' vs ii' and i' vs iii'; F i' vs ii'). Indeed, depletion of *dPI4KIIIα, dTTC7, or stmA* using *nubbin*-Gal4 resulted in a complete absence of the adult wing though there were wing discs present in this genotype in late pupal stages (supplementaryFig3 Ai vs ii, A i vs iii and Ai-iv). Since we observed cell death in each of the pupal or larval wing disc compartments when *dPI4KIIIα* was depleted, we attempted to rescue this phenotype by expression of *Death-associated inhibitor of Apoptosis* (DIAP1). DIAP1 is an E3 ubiquitin ligase with caspase inhibitor activity and thus can prevent apoptotic cell death (Wang et al., 1999). When DIAP1 was ectopically expressed in *ptc* > *dPI4KIIIα*^{i} cells, a partial rescue of the L3-L4 inter-vein was observed, thus supporting the role of apoptosis in driving the reduced L3-L4 inter-vein distance in *ptc* > *dPI4KIIIα*^{i} (Supplementary Fig2 C i vs iv and graph D). Ectopic expression of DIAP1 did not have effect on the adult wing (supplementary Fig. 2Ciii).

2.7. Hedgehog signalling appears unaffected following dPI4KIIIα depletion in larval wing discs

An alternate possibility to explain the reduced L3-L4 inter-vein distance in *ptc* > *dPI4KIIIα*^{i} is reduced *hh* signalling (Vervoort et al., 1999).

Fig. 2. Changes in plasma membrane PI4P levels observed upon *dPI4KIIIα* complex knockdown.
Ai and iii) Confocal images of S2R + cells transiently transfected with pUAST-P4M::GFP attB plasmid and reagent control respectively. **Aii and iv)** Corresponding DIC images of the same cells. 20–25 cells were checked for expression of the probe. 48 hr post transfection live cells were imaged for GFP, n = 20 cells. **B)** Western blot from the same set of transfected cells showing the expression of the correct sized GFP tagged P4M protein. Anti GFP antibody was used for detection of P4M::GFP. The experiment was repeated twice and one such set is reported. **Ci and ii)** *ptc* > P4M::GFP probe alone and *ptc* > *dPI4KIIIα*^{i}, P4M::GFP probe in the third instar larval wing disc. The cartoon in the inset shows third instar wing disc; *ptc-gal4* domain is marked by white line and the rectangle marks the region used for analysis. **D)** Quantification of fluorescence intensity in wild type and *dPI4KIIIα* knockdown backgrounds. 5–6 discs per genotype were used and 10–20 cells per wing disc were used for quantification. The experiment was repeated twice, and one set is reported here. **Ei, ii and iii)** Representative wing images of the control, *dPI4KIIIα*^{i} alone and the same RNAi along with the PI4P probe P4M::GFP respectively. Note that the phenotype is not modulated by presence of the PI4P probe (compare ii and iii) n = 5 for each genotype. Scale bar is 10 μm.

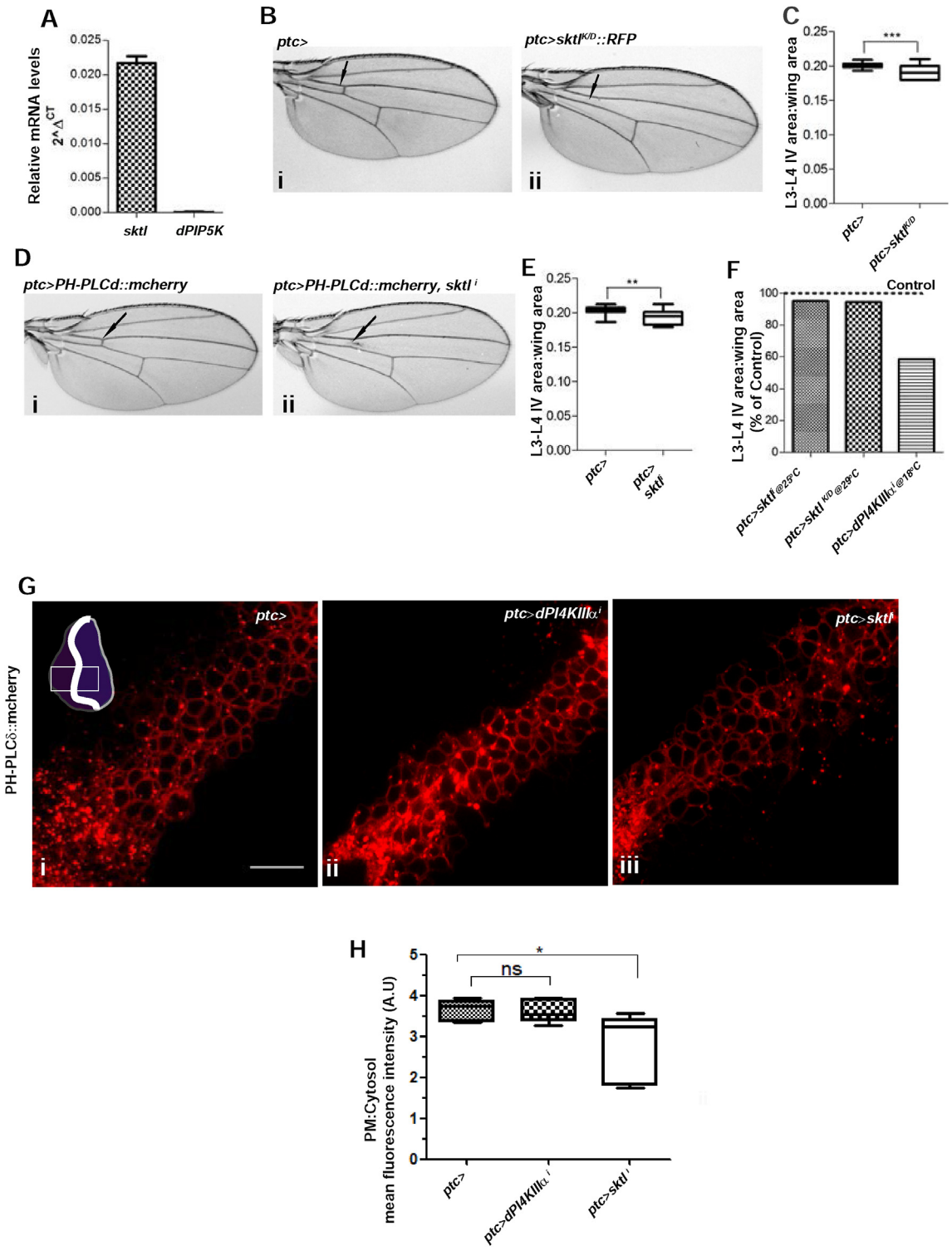

Fig. 3. Venation defect seen upon *dPI4KIIIα* complex knockdown is distinct from changes in PI(4,5)P_2 levels.
A) q-PCR based detection of transcripts of different PIP5Ks, *sktl,* and *dpip5k* with respect to RP49 transcripts in the wild type wing disc. The experiment was repeated twice and result of one such experiment is reported here. **Bi and Di)** Control wing images. **Bii and Dii)** Overexpression of kinase dead *sktl* ($sktl^{K/D}$) and *sktl* knockdown ($sktl^{i}$) respectively with the consequent venation defect marked by black arrows. **C and E)** Quantification of the L3-L4 inter-vein distance in case of $sktl^{K/D}$*::RFP* over expression and $sktl^{i}$ mediated knockdown. For all adult wings experiment n $\geq$ 10. **F)** Comparison of severity of shortening of L3-L4 inter-vein distance in case of different genetic manipulations of *sktl* and *dPI4KIIIα*. **Gi, ii, iii)** Representative images of wing discs expressing the PI(4,5)P_2 probe PH-PLCδ:mCherry in wild type, *dPI4KIIIα* knockdown and *sktl* knockdown using the *ptc* driver at 25 °C. Inset carton is a third instar wing disc; white line is the *ptc* domain and rectangle marks the area from which cells were used for analysis. The scale bar represents 10 μm. H) Quantification of PH-PLCδ:mCherry fluorescence intensity.

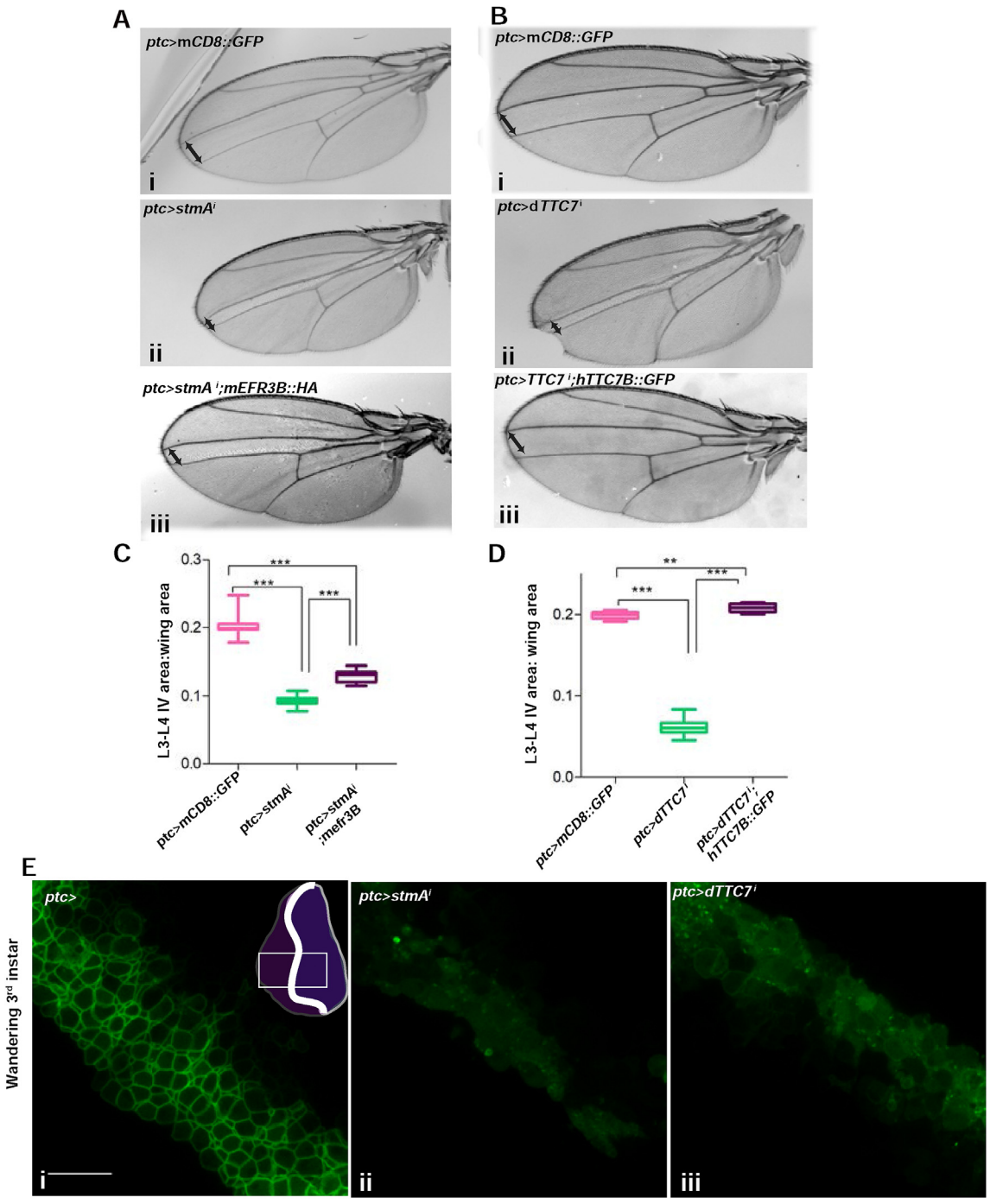

Fig. 4. dTTC7 and StmA work in conjunction with dPI4KIIIα to affect venation patterning.
Ai and Bi)*ptc*-Gal4 controls. **Aii and Bii)** Wings of *ptc* > Efr3/*stmA*^{i} and *ptc* > *dTTC7*^{i} RNAi respectively. The inter-vein area as well as the ACV region show defects as seen in *ptc* > *dPI4KIIIα*^{i} wings in the same domain. **Aiii)** Partial rescue of the *stmA*^{i} phenotype with mouse ortholog of Efr3 (mEFR3B). **Biii)** Rescue of the *dTTC7*^{i} phenotype with the human ortholog hTTC7B. **C and D)** Quantification of the shortening of the inter-vein and the partial rescue for *stmA* and *dTTC7* respectively. **Ei, ii and iii)** Third instar wing discs expressing P4M::GFP in wild type, *stmA*^{i}, and *dTTC7*^{i} driven by *ptc*. The inset cartoon shows the third instar wing disc with the white line marking the *ptc* domain and rectangle the area from which cells were chosen for analysis. Since there was no enrichment of the probe in plasma membrane of the *ptc* > *dTTC7*^{i} and *ptc* > *stmA*^{i}, it was not possible to quantify it. Scale bar is 10 μm.

To test if *hh* signalling in wing discs is disrupted we employed two commonly used readouts to measure outputs of *hh* signalling. As a positive control for our assays, we overexpressed *ptc*, a negative regulator of *hh* signalling (Forbes et al., 1993) in the *ptc* domain in *ptc* > *ptc::YFP* flies and found that the L3-L4 inter-vein distance was reduced (supplementary Fig 3Ai, ii graph B). To test if *hh* signalling in wing discs is disrupted we used two reporters commonly used to measure outputs of the *hh* signalling pathway, namely the protein levels of Ptc, the transmembrane receptor of *hh* and Ci (a member of the Gli family of transcription factors) (Forbes et al., 1993; Von Ohlen et al., 1997). We performed immunofluorescence staining to detect the levels and distribution of Ptc and Ci proteins in 3rd instar larval wing discs as defects in *hh* signalling are usually detectable at this stage. In *ptc* > *ptc::YFP* discs, Ptc staining was more intense as expected but spanned a smaller region of the wing disc

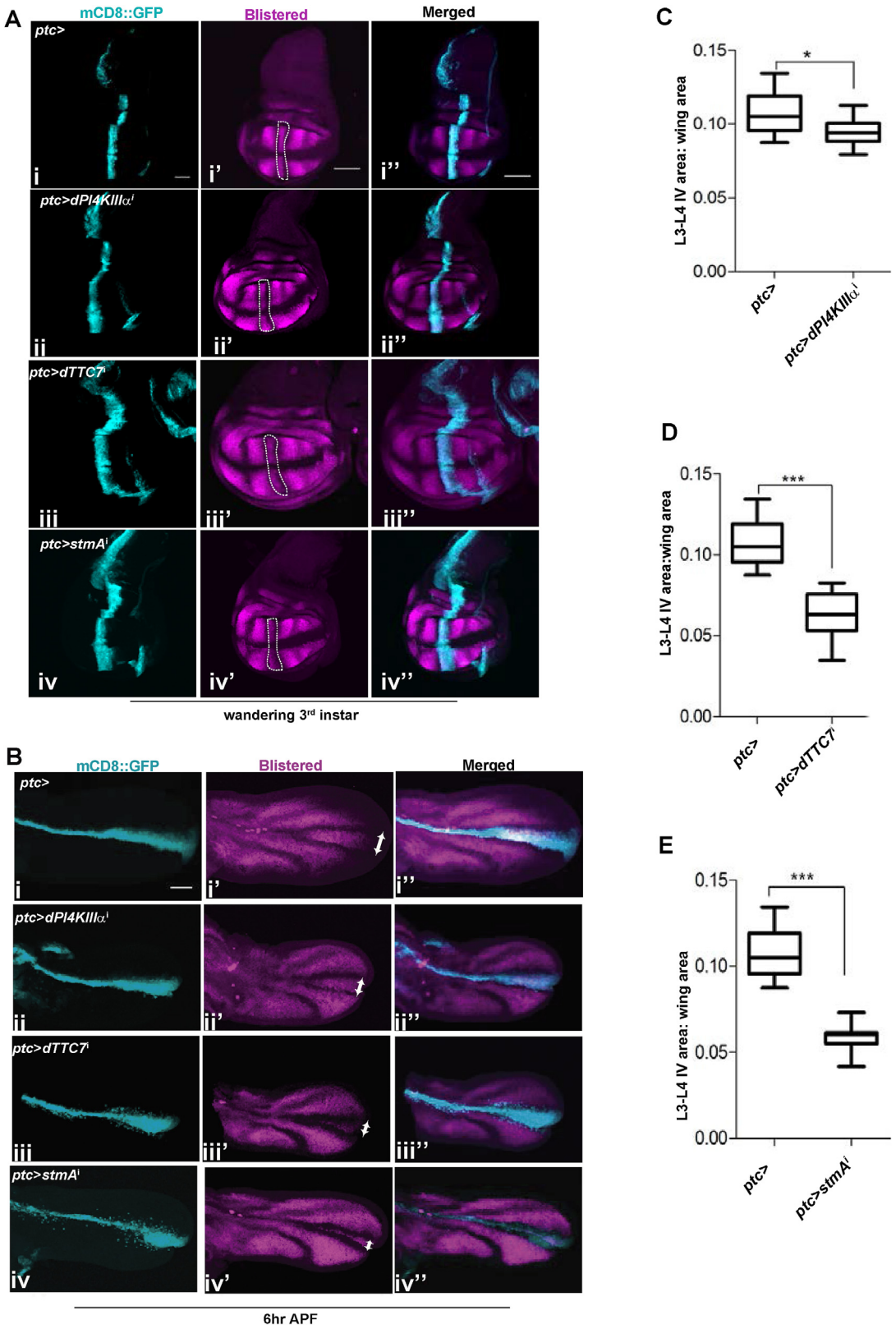

Fig. 5. Developmental timing of the venation defect.
Ai-iv and Bi-iv) represent *ptc* > mCD8::GFP to denote the region of RNAi manipulation. **Ai'-iv')** Discs stained with Blistered antibody marking all the inter-vein cells and making the pro-veins visible by negative staining (n = 10 for each genotype and the experiment was repeated thrice with the figure representing data from one such trial). Note there is no detectable difference between control (**Ai')** and the RNAi manipulated (**Aii'-iv**') discs. The region of interest i.e., the presumptive L3-L4 inter-vein is marked by white dotted lines. **Bi'-iv')** Blistered staining in indicated genotype at 6 h after pupae formation (APF). Developmental time point is mentioned below the figure panel and genotype of each wing is mentioned within each panel. Bii'-iv' wings have smaller L3-L4 distance (marked by white arrowhead) as compared to Bi' (control). **Ai''-iv'' and Bi''-iv'')** Merged images. **C, D, E)** Quantifications of the L3-L4 inter-vein distance of d*PI4KIIIα, dTTC7* and *stmA* RNAi at 6 h APF (The experiment was repeated thrice and n = 10 for each genotype). Scale bar is 50 μm.

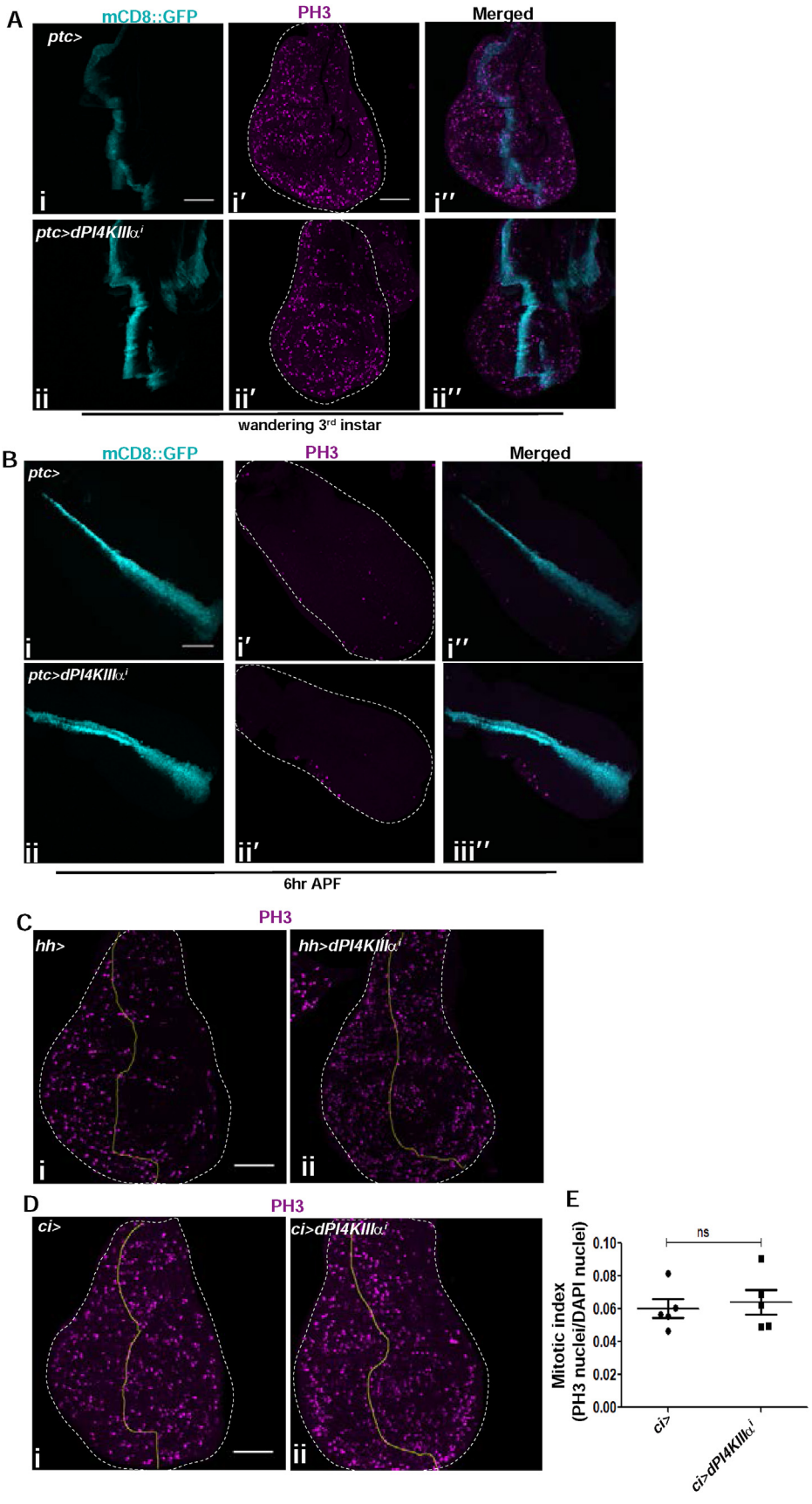

Fig. 6. Depletion of *dPI4KIIIα* during development does not affect cell division. A, B) Anti phosphohistone 3 (PH3) staining for third instar and 6 h APF wing discs respectively. **Aii and Bii)** *ptc* > *dPI4KIIIα*^{i}**Ai and Bi)** Corresponding controls. The experiment was repeated twice, n = 8 for control and n = 10 for RNAi genotype. **C i, ii and Di, ii)** Anti PH3 stained third instar larval wing discs driving *dPI4KIIIα* depletion in the *hh* and *ci* domains respectively. Ci and Di are the controls and Cii and Dii are *ci* > *dPI4KIIIα*^{i} and *hh* > *dPI4KIIIα*^{i} depleted discs, respectively. The yellow line demarcates the anterior and posterior compartments. The boundaries of wing discs are denoted by white dotted line. Posterior is to the left. Scale bar is 50 μm. **E** Mitotic Index of ci and *ci* > *dPI4KIIIα*^{i} 3rd instar wing discs is represented. Y-axis shows the mitotic index calculated as described in methods. Genotypes represented on X-axis. Each point represents the index as calculated from a single disc, error bars indicate standard error of mean (SEM). n = 5 discs per genotype.

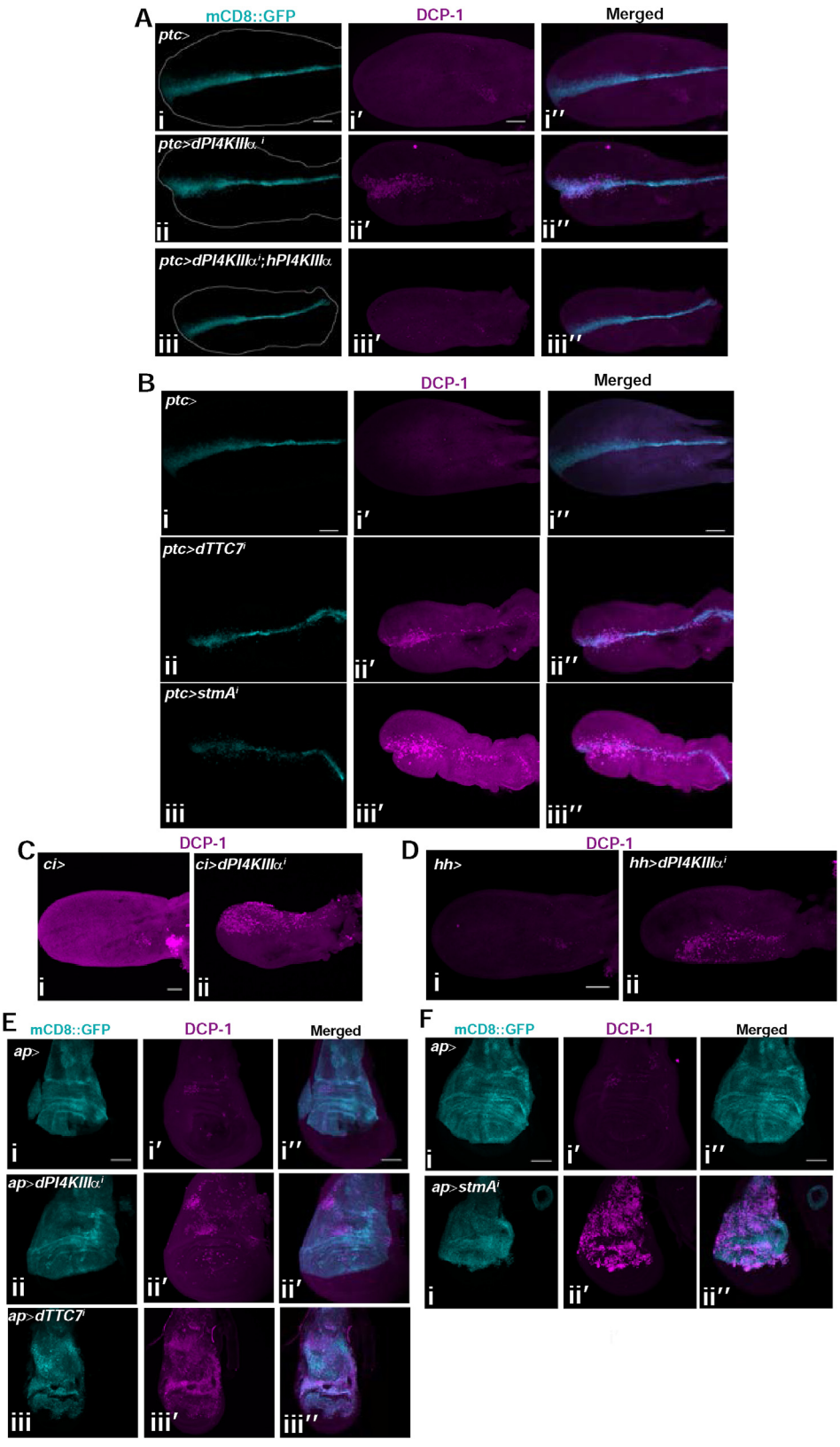

Fig 7. Depletion of the components of dPI4KIIIα complex causes cell death by apoptosis. All the wing discs are stained with apoptosis marker Dcp-1 (Drosophila Caspase 1). **Ai-Fi)** Regions showing *dPI4KIIIα*, *stmA,* and *dTTC7* RNAi manipulation by corresponding Gal4 drivers. **A-D)** Pupal wing discs (5.5–6 h APF). **Ai'-Fi')** Corresponding controls. **Aii')** *ptc > dPI4KIIIα^{i};* **Aiii')** *ptc > dPI4KIIIα^{i}; hPI4KIIIα* pupal wing discs (5.5–6 h APF). Aii' wing discs are Dcp-1 positive while in the rescue genotype of Aiii there is no Dcp-1 staining. **Bi)** Control, **Bii' and iii')** *stmA* and *dTTC7* RNAi in the *ptc* domain. Bii' and iii' stain positive for Dcp-1. **Ci')** Control, **Cii')***ci > dPI4KIIIα^{i}*. **Di')** Control, **Dii')** *hh > dPI4KIIIα^{i}*. **E-F)** Third instar larval wing discs stained with antibody against Dcp-1. **Ei')** Control, **Eii' and iii')** *ap > dPI4KIIIα^{i}* and *ap > dTTC7^{i}*. Crosses in experiment E were carried out at 29 °C for maximal knockdown of the genes concerned. **Fi')** Control, **Fii')** *ap > stmA^{i}*. Crosses in experiment F were carried out at 25 °C as 29 °C did not yield viable larvae. Scale bar is 50 μm.

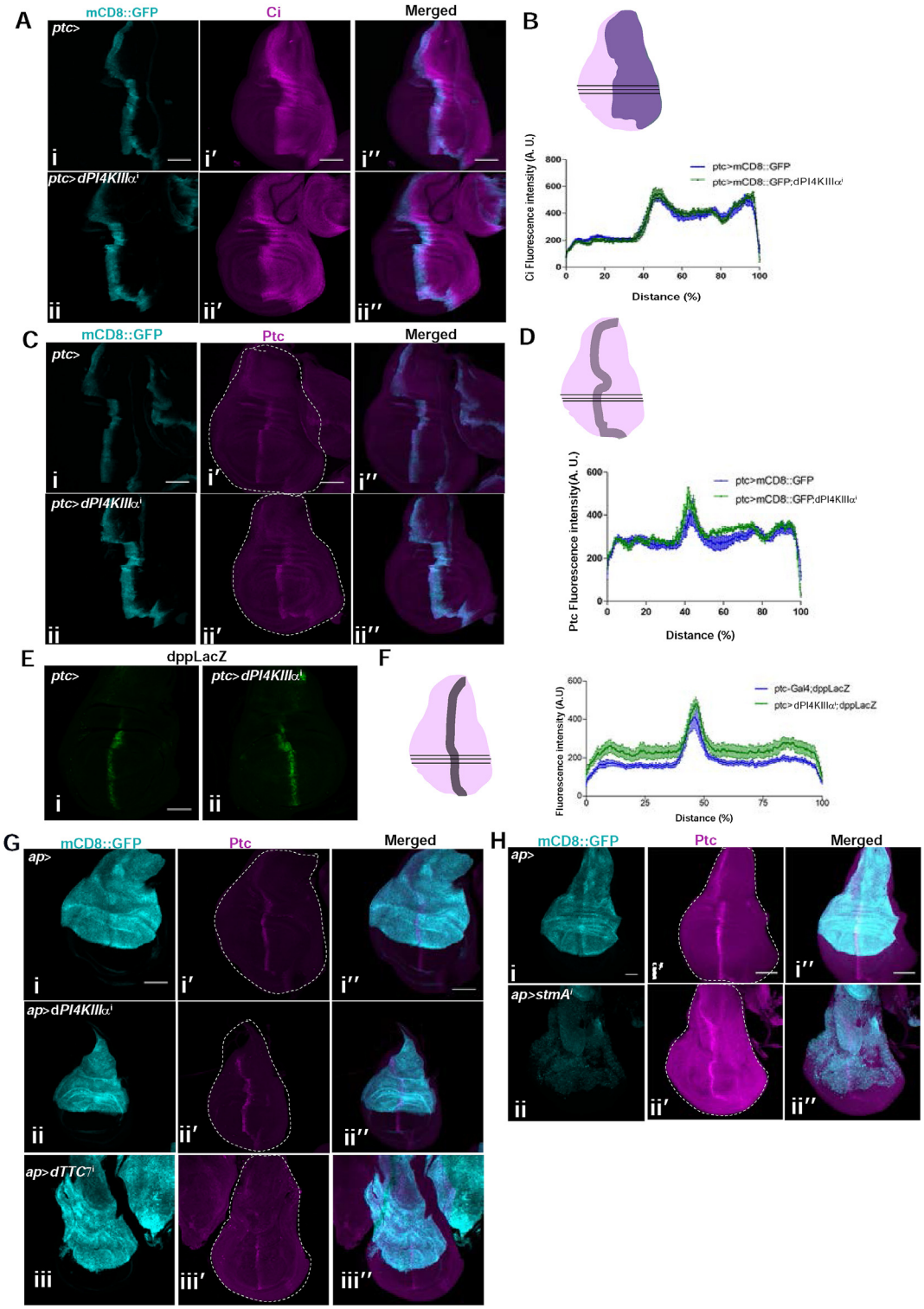

Fig. 8. Depletion of dPI4KIIIα complex shows no effect on the readouts of hedgehog signalling in larval stages.
Ai-ii and Ci-ii) Third instar wing disc images showing expression of *ptc* > mCD8::GFP. **Ai'-ii' and Ci'-ii')** Same discs stained for Ci and Ptc in control and ptc > *dPI4KIIIα*^{i}, respectively. All discs are positioned with anterior to the right and posterior to the left. **Ei and ii)** Third instar wing disc of control and ptc > *dpi4KIIIα*^{i}, respectively stained for lacZ antibody to show the expression pattern of Dpp-lacZ. Three repeats for each staining was done and n = 7–10 for each genotype. **B, D, F)** Quantification of spread of indicated antigens, with 6–7 discs used per experiment. The quantification was repeated thrice with three different biological sets. **G and H)** Data with *ap Gal4* driver. **Gi-ii and Hi-ii)** Third instar wing disc images showing expression of *ap* > mCD8::GFP to demarcate region of RNAi manipulation. **Gi'-ii' and iii')** Same discs stained for the Ptc in control, *ap* > *dPI4KIIIα*^{i} and *apt* > *dTTC7*^{i} respectively. **Hi'-ii')** Same discs stained for the Ptc in control and *apt* > *stmA*^{i} respectively. All experiments were repeated thrice. For the graphs B, D and F the regions of the wing disc chosen and the line profiles for intensity measurements are depicted by cartoons in corresponding panels. White dotted lines mark the wing disc boundaries. Scale bar is 50 μm.

(supplementary Fig 3Bi', ii' and graph D) and the intense staining band of Ci was also reduced (supplementary fig 3B iii', iv' and graph E). Both these changes are indicative of attenuated *hh* signalling. However, when compared to controls we did not detect any change in either Ci (Fig. 8Ai', ii' and graph B) or Ptc (Fig. 8Bi', ii' and graph D) staining between the control and *ptc > dPI4KIIIα*^{i}. We also checked for perturbation in Dpp production using a *dpp-lacZ* strain in the background of *ptc > dPI4KIIIα*^{i}. Once again, compared to controls (Fig. 8Ei, ii and graph F), there was no obvious difference in *dpp-lacZ* expression between *ptc > dPI4KIIIα*^{i} and control larval discs. Since we did not see any indication of reduced *hh* signalling using this driver, we further tested the effect on *hh* signalling when the *ap*-GAL4 driver that expresses only in the dorsal wing disc encompassing both the anterior and posterior compartments was used. In case of depletion, i.e *ap > dPI4KIIIα*^{i} (see Fig. 8Gi' vs ii'), *ap > dTTC7*^{i} (Fig. 8Gi' vs iii') as well as *ap > stmA*^{i} (Fig. 8Hi' vs ii') we did not detect any alteration in Ptc staining indicative of perturbed *hh* signalling. Moreover, we stained for Ci in both *ap > dPI4KIIIα*^{i} and *ap > dTTC7*^{i} third instar larval wing discs and no difference in Ci staining pattern was observed between control, *dPI4KIIIα* and TTC7 depleted wing discs (supplementary Fig 4Ai' vs ii' and Bi' vs ii'). The positive control *ap > Ptc::YFP* discs had no Ci staining in the region of Ptc overexpression (supplementary Fig 2 Bi' vs iii').

3. Discussion

The plasma membrane of cells composed of both proteins and lipids is an interface with the extracellular environment and plays an important role in interpreting extracellular signals. The proteins of the plasma membrane include receptors such as those that bind developmental signals like hormones and morphogens as well as channels and transporters. Several lipids including PI(4,5)P_2 and PI4P are enriched at the plasma membrane and may be important for protein function (Hilgemann et al., 2018). While PI(4,5)P_2 has been shown to regulate the function of several plasma membrane proteins [reviewed in Hille et al. (2015); Martin (2015); Posor et al. (2015)], PI4P has largely been considered as a substrate for the synthesis of PI(4,5)P_2. Independent of their ability to regulate protein activity, PI4P and PI(4,5)P_2 are also thought to be essential determinants of the plasma membrane. Although, it has recently been suggested that the negative charges on these lipids may regulate plasma membrane protein activity (Hammond et al., 2012), the impact of such regulation on cell and tissue function has remained unknown. In this study, we found that depleting the dPI4KIIIα protein complex in specific domains of the developing wing resulted in defective venation pattern in the adult wing. Importantly, we found that when dPI4KIIIα was depleted in *ptc-Gal4* domain cells, the levels of plasma membrane PI4P were reduced while PI(4,5)P_2 levels were not altered. This observation strongly suggests that PI4P itself is required to mediate cellular functions at the plasma membrane of *ptc-GAL4* cells. Together with our finding that PI(4,5)P_2 levels are not altered in *ptc-GAL4* domain cells on dPI4KIIIα depletion, our observations suggest a role for dPI4KIIIα in generating a pool of PI4P in these cells that is required for wing development. Interestingly and in contrast to this study, previous work in *Drosophila* has demonstrated a role for dPI4KIIIα in regulating plasma membrane PI(4,5)P_2 in adult photoreceptors for PLC signalling (Balakrishnan et al., 2018) and for PI(4,5)P_2 dependent processes in the developing female germline (Tan et al., 2014). These differences in the requirement of PI4KIIIα may reflect differences in distinct cell types with respect to their PI4P generated plasma membrane PI(4,5)P_2 pools. Previous work has shown that with respect to PI(4,5)P_2, there exist multiple pools of this lipid dedicated to distinct functions at the plasma membrane [(Chakrabarti et al., 2015) and reviewed in Kolay et al. (2016)]. In the case of plasma membrane PI4P too, there may be multiple pools of this lipid, only some of which may be required for PI(4,5)P_2 synthesis; these may vary between cell types and may have distinct functions.

PI4KIIIα has been shown to exist as a complex of at least three proteins (PI4KIIIα, stmA/Efr3 and TTC7) at the plasma membrane in yeast and mammalian cells (Baird et al., 2008; Nakatsu et al., 2012) and this has also been recently shown in *Drosophila* photoreceptors (Balakrishnan et al., 2018). While this suggests an equivalence in phenotypes on depletion of these proteins *in vivo*, the reported consequence of depleting each of these components in animal models seems variable. It is reported that mutations in human PI4KIIIα are associated with neurodevelopmental defects and late gestational lethality (Pagnamenta et al., 2015). By contrast, mutations in TTC7A result in a range of intestinal defects including atresia, inflammatory bowel disease, dermatological disease, and severe immunodeficiency (Mandiá et al., 2018) and mutations in Efr3A have been linked to neural degeneration (Hu et al., 2017) and autism spectrum disorder (Gupta et al., 2014). Although depletion of each of these proteins has been shown to affect plasma membrane PI4P levels in cultured mammalian cells, these varied phenotypes when they are depleted raise questions on the function of these three proteins in equivalent cellular processes *in vivo*. In this study, we found that depletion of dPI4KIIIα, Efr3, and TTC7 individually in *ptc-GAL4* domain cells results in identical defects in wing patterning suggesting that all three proteins not only regulate PI4P levels *in vivo* but also impact equivalent signalling events resulting in comparable phenotypic outcomes. In mammalian models, additional proteins TMEM150A (Chung et al., 2015) and FAM126A (Baskin et al., 2016) have been implicated as additional protein regulators of dPI4KIIIα function but orthologs of TMEM150A have not been found in non-mammalian genomes such as yeast and *Drosophila*. It is possible that the presence of such additional proteins in the dPI4KIIIα complex of mammalian cells results in functionally different pools of this enzyme thus contributing to phenotypic variability *in vivo*. Nonetheless our observation of equivalent phenotypes on depleting dPI4KIIIα, dTTC7 and StmA in *ptc-GAL4* cells (this study) and photoreceptors (Balakrishnan et al., 2018) strongly underscores the model that these three molecules are part of a core protein complex that regulates not only PI4P levels at the plasma membrane but also signalling outcomes resulting from the function of this complex.

The reduction of L3-L4 inter-vein area that we observed on dPI4KIIIα depletion is a well-known phenotype associated with reduced *hh* signalling and altered hh signalling on dPI4KIIIα depletion has been reported by a previous study (Yavari et al., 2010). However, surprisingly and in contrast to those studies, we found that canonical readouts of *hh* signalling including Ptc and Ci protein distribution and dpp-lacZ levels were not altered in *dPI4KIIIα* depleted wing-discs. Indeed, we found that depletion of *dPI4KIIIα* in the *ap*-GAL4 domain [such as performed by Yavari et al. (2010)], also did not affect readouts of *hh* signalling in the developing wing though we have used highest level of knockdown (for example with experiments at 29 °C) and more efficient RNAi lines whose ability to reduce PI4P levels at the plasma membrane of wing disc cells are clearly demonstrated. Even with the RNAi lines used by Yavari et al., we did not observe changes in Ptc staining (data not shown). Under the same assays, we were able to detect changes in *hh* signalling using well-established methods such as *ptc* overexpression. Thus, overall our studies do not support a role of dPI4KIIIα in mediating *hh* signalling in *ptc* domain cells of the developing wing disc.

Given that we did not find altered *hh* signalling when dPI4KIIIα was depleted, what might explain the altered venation pattern and morphological defects in these wings? Reduced cell divisions or increased death during development could contribute to the wing defects in adult wings. In zebra fish embryos, morpholino mediated depletion of PI4KIIIα did show a reduction in number of dividing cells (Ma et al., 2009). Contrary to this, we did not observe significant differences in cell divisions between control and *dPI4KIIIα* depleted wing discs in the anterior, posterior or cells apposing the A/P boundary (Fig. 6A, C and D). During the course of development, cell divisions in the wing discs gradually organise themselves into territories around the inter-vein regions while presumptive vein tissues do not show actively dividing cells (Milán et al., 1996). In our experiments with 6 h APF pupal wing discs (Fig. 6B i' v ii'), PH3 staining was comparable between controls and *ptc > dPI4KIIIα*^{i}suggesting that defects in cell division do not underlie the reduced

L3-L4 inter-vein area. An alternative possibility is that reduced dPI4KIIIα activity results in enhanced cell death resulting in the decreased L3-L4 inter-vein area and other wing morphological defects.

A role of phosphoinositides in mediating cell death is an emerging field of study and till date, the function of the phosphoinositide 3 kinase activated pro-survival signal AKT is the most well studied [reviewed in (Phan et al., 2019)]. Direct involvement of phosphoinositides in regulating apoptosis comes from *in-vitro* studies which demonstrated that PI(4,5)P_2 containing micelles can inhibit both initiator and effector Caspases (Mejillano et al., 2001). In fact, a role of PI4Ks in mediating apoptosis in different cell types via the AKT driven phosphorylation of Caspases in the context of EGF stimulation is documented for PI4KIIα (Kme et al., 2010). Consistent with these pieces of evidence, we found enhanced Dcp-1 staining in *ptc* > *dPI4KIIIα*^{i} cells as well as in *hh*-GAL4 and *ci*-GAL4 domain cells when any of the three components of the dPI4KIIIα complex was depleted. Indeed, depletion of dPI4KIIIα complex components using *ap*-GAL4 results in enhanced cell death despite not affecting *hh* signalling outputs such as Ptc expression. Our finding that this apoptotic cell death could only be partially be reversed by expression of the cell death inhibitor DIAP1 may reflect the relatively weak effect of reagents available to inhibit this process; alternatively, they may also imply other ongoing processes contributing to cell death (apart from apoptosis) in PI4KIIIα depleted cells; these remain to be identified.

The developing wing disc in *Drosophila* has regenerative potential which decreases with progression of development and discs injured in the late third instar or pupal period do not show regeneration (Harris et al., 2016). This is borne out in our experiments where Dcp-1 induced cell death results in a morphologically defective adult wing wherever viable progeny is obtained after dPI4KIIIα depletion. These findings strongly suggest that the dPI4KIIIα complex is required to inhibit cell death and hence ensure cell viability in the developing wing, a role consistent with the proposed key role of PI4P as a lipid determinant of the plasma membrane. Our model is consistent with and provides a possible cellular mechanism for the observation that null mutations in *Drosophila* PI4KIIIα (Tan et al., 2014; Yan et al., 2011) and *stmA* (Huang et al., 2004) are cell lethal, null yeast mutants in these genes are non-viable and PI4KIIIα knock out mice are embryonic lethal (Nakatsu et al., 2012). Overall our work provides evidence for an important role of the PI4P produced by the dPI4KIIIα complex in supporting cell viability in a developmental context. The specific molecular mechanisms by which PI4P supports cell viability remain to be understood.

4. Materials and methods

4.1. Fly culture and genetics

Flies (*Drosophila melanogaster*) were maintained on regular medium containing corn flour, sugar, yeast powder and agar along with antibacterial and antifungal agents. Genetic crosses were reared at 18 °C (for all *PI4KIIIα*, *TTC7* and *stmA* phenotyping), 25 °C (for *sktl* RNAi and all other developmental timing experiments and *ap* > *dstmA*^{i}) or 29 °C (for *sktl* kinase dead, *ap* > *dPI4KIIIα*^{i}, and *ap* > *dTTC7*^{i}) and as and when required (indicated in conjunction with specific results). There was no internal illumination within the incubator.

Red Oregon-R (ROR) was the wild-type strain. The details of the fly alleles and insertions obtained for the experiments are described here: *PI4KIIIα*^{RNAi} (BDSC:38242), (VDRC:v15993 and v105614), *TTC7*^{RNAi} (BDSC:44482), (VDRC:v35881), *stmA*^{RNAi} (VDRC:v47751), *ptc*^{RNAi} (BDSC:2879),UAS-smo.C.MycMyr (BDSC:44617), UAS-ptcYFP37C, *ptc* –Gal4 (NCBS fly stock centre), *hh*^{mrt} (BDSC:26166), *ci*-Gal4, *hh*-Gal4 (Satyajit Mayor lab, NCBS), UAS-3xFLAG::hPI4KIIIα, UAS-h*TTC7*B::GFP, UAS-me*fr3*B::HA, UAS-P4M::GFP, UAS-4c-PLCd1PH::mCherry (Patrik Verstreken lab). BDSC is Bloomington Drosophila Stock Center and VDRC is Vienna Drosophila Research Consortium respectively.

4.2. Cell culture

S2R + cells were maintained in Schneider's *Drosophila* medium (SDM; 21720024, Gibco, Thermo Fisher Scientific) supplemented with 10% heat inactivated fetal bovine serum (FBS; 1600044, Gibco, Thermo Fisher Scientific) and penicillin-streptomycin-glutamine (10 ml/l; G1146, Sigma-Aldrich), with puromycin as a selection agent. The cells were maintained at 23 °C and passaged regularly.

4.3. Adult Drosophila wing imaging

Adult female flies of correct genotypes were dipped in 70% ethanol, briefly dried and wings clipped. The adult wings were mounted in colourless nail varnish and imaged under a light microscope (Olympus SZX12). Quantification of the area was done by stitching images of multiple wings to generate a stack and manually delineating the area using ImageJ. Graphs were generated using GraphPAD Prism5.

4.4. Western immunoblotting

S2R + cells stably transfected with actin-gal4 were used. 0.5 μg DNA of pUAST-P4M::GFP plasmid was used for transient transfection using Effectene (301425, Qiagen). 48 h post transfection cells were dislodged from wells and washed in 1X phosphate buffered saline (PBS) twice following which the cell pellet was homogenized in 2× SDS-PAGE sample buffer followed by boiling at 95 °C for 5 min. Samples were separated using SDS-PAGE and electro blotted onto nitrocellulose membrane (Hybond-C Extra; GE Healthcare) using semidry transfer assembly (Bio-Rad) for 30 min at 15 V. Following blocking with 5% Blotto (sc-2325, Santa Cruz Biotechnology) for 2 h, blots were incubated overnight at 4 °C in appropriate dilutions of primary antibodies [anti-α-tubulin [1:5000 dilution; E7 Developmental Studies Hybridoma Bank (DSHB)], anti-GFP [Santa Cruz # sc-9996 (1:2000 dilution)]. Following incubation with primary antibody the blots were washed in PBST (1XPBS + 0.1% Tween 20) and incubated with appropriate horseradish peroxidase coupled secondary antibody (Jackson Immuno Research Laboratories) in 1:10,000 dilution for 2 h at room temperature. Following further washes, blots were developed with ECL (GE Healthcare) and imaged using a LAS 4000 instrument (GE Healthcare).

4.5. RNA extraction and qPCR

RNA was extracted from *Drosophila* ROR wing disc using TRIzol reagent (15596018, Life Technologies). Post purification, RNA was treated with amplification grade DNase I (18068015, Thermo Fisher Scientific) and cDNA synthesis was performed using SuperScript II RNase H–Reverse Transcriptase (18064014, Thermo Fisher Scientific) and random hexamers (N8080127, Thermo Fisher Scientific). Quantitative PCR (qPCR) was carried out using Applied Biosystem 7500 Fast Real Time PCR instrument. Primers were designed at the exon-exon junction following the parameters recommended for qPCR. Across samples transcript level of the ribosomal protein 49 (RP49) was used for normalization. Two different biological replicates were used, and each sample was measured in triplicates to ensure the consistency of the data. GraphPAD Prism5 was used for plotting the graph. The primers used were as follows:

RP49:fwd:5'CGGATCGATATGCTAAGCTGT3'; RP49rev:5'GCGCTTGTTCGATCCGTA3';*sktl*fwd:5'CTCATGTCCATGTGTGCGTC; *sktl* rev:5'TTAATGGTGCTCATCAGTG3';*dPIP5K* fwd:5'AGCAGAGAAAACCGCTTAGG3'; *dPIP5K* rev:5'GGCGATTCACTGACTTATTCC3'.

4.6. Immunohistochemistry

For checking expression of P4M::GFP in S2R + cells, cells were transfected using above mentioned protocol (see Western

immunoblotting) and 48 h post transfection cells were dislodged from wells and plated in coverslip along with fresh Schneider's complete medium and incubated at 23 °C for 2 h following which they were imaged using confocal microscope (Olympus FV1000). For immunofluorescence, wing discs from wandering 3rd instar larvae and 6 h APF pupae were dissected under light microscope in (PBS) and then fixed in 4% paraformaldehyde in PBS for 20 min at room temperature (~25 °C). Fixed discs were washed 3 times in PBTx (PBS with 0.3% TritonX-100) for 5 min each time. The tissues were then incubated in blocking solution [5% normal goat serum (NGS; 5425, CST) in PBTx] for 30 min at room temperature, after which the tissues were incubated overnight at 4 °C with primary antibodies diluted in blocking solution Following antibodies were used: anti-Ptc 1:40 (Apa 1.3, DSHB), anti-Ci–1:10 (2A1, DSHB), anti-beta galactosidase 1:10 (40-1a, DSHB), anti-blistered-1:200 (kind gift from Professor Seth Blair's Lab), anti PH3 (1:200, Merck), cleaved *Drosophila* DCP-1 (1:200, CST #9578). Appropriate fluorophore conjugated secondary antibodies were used at 1:200 dilutions in blocking solution [Alexa Fluor 633/568 IgG, (Molecular Probes)] and incubated for 1.5 h at room temperature. After three washes in PBTx, the tissues were washed in PBS for 5 min, mounted in mounting medium [Prolong Gold or Prolong Diamond (Thermo Fisher Scientific)] and cured for required time. The whole-mounted preparations were viewed under Olympus FV1000 laser scanning confocal microscope and ImageJ was used for quantification.

4.7. Imaging PI4P and PI(4,5)P_2 levels

Third instar larval wing disc cells were used for measuring PI4P amd PI (4, 5)P_2. These phosphoinositide measurements were carried out using P4M::GFP and PH-PLCδ::mCherry probe for PI4P and PI(4,5)P_2 probes respectively. Wandering third instar larvae were carefully selected, dissected, and mounted in Schneider's *Drosophila* medium (SDM; 21720024, Gibco, Thermo Fisher Scientific) followed by live imaging in the Olympus FV3000 confocal microscope. z stacks of the cells in same plane were manually selected, maximum intensity projection of summed z stack was obtained and plasma membrane to cytosolic fluorescence ratio was calculated for individual cells by drawing line profiles using ImageJ. 10–20 cells were analysed per wing disc and 5-6discs per genotype was quantified. Thus, on an average 50–60 cells per genotype were analysed to obtain the data. The software GraphPAD Prism5 was used for plotting the graphs.

4.8. Quantification of Ptc, Ci and Dpp lacZ

Wandering third instar wing discs from respective genotypes were fixed, stained and imaged as mentioned above. Maximum intensity z-projections were created manually by summing of the z-optical slices from individual wing discs and stacks were made of 5–6 discs for each genotype. Multiple (three) line profiles were drawn above the dorso-ventral boundary by manually selecting the boundary. Each line profile was of 3-pixel width and spanned the entire length of the disc. Raw X (distance) and Y (intensity)coordinates were obtained by using the plot profile function in ImageJ. The X coordinates were converted into % of the length of each disc and binned into values from 0 to 100. Corresponding Y values for each bin was averaged and multiple such data points for each disc from different line profiles were averaged to obtain the mean intensity of staining of a single disc. This entire measurement was then carried out on 5–6 discs for each genotype. The resultant mean from each disc was then plotted using GraphPad prism to generate XY-line graphs with SEM.

4.9. Mitotic index measurement

Third instar larval wing discs of *ci>* and *ci > dPI4KIIIα*^{i} were carefully staged and dissected. The discs were then stained with DAPI (1:10000), anti PH3 (1:200) and anti-Smo (1:40) to mark the total number of nuclei, dividing nuclei and compartment boundary respectively. The anterior wing pouch was selected and total n umber of nuclei and dividing nuclei were measured. A ratio of dividing nuclei to total nuclei was plotted and this was then plotted using Graphpad Prism to obtain the mitotic index.

4.10. Statistical analysis

For quantification involving more than two biological groups one-way ANOVA was used for determining statistical significance followed by post hoc Tukey's comparison test between each pair of genotypes. For graphs involving two genotypes Mann-Whitney test was used without assuming a normal distribution.

Symbol	Meaning
ns	$P > 0.05$
*	$P > 0.05$
**	$P \leq 0.01$
***	P 0.001
****	$P \leq 0.0001$ (For the last two choices only)

Funding

We acknowledge support of the Department of Atomic Energy, Government of India, under project no. 12-R&D-TFR-5.04-08002 and 12-R&D-TFR-5.04-0900. This work was supported by the National Centre for Biological Sciences-TIFR (core), a Wellcome DBT India Alliance Senior Fellowship to PR (IA/S/14/2/501540) and a studentship from the Council for Scientific and Industrial Research-India to UB.

Acknowledgments

We thank the NCBS Imaging Facility and Fly Facility for support during this project and numerous colleagues for sharing reagents including fly stocks and antibodies.

Appendix A. Supplementary data

Supplementary data to this article can be found online at https://doi.org/10.1016/j.ydbio.2020.03.008.

References

Altan-Bonnet, N., Balla, T., 2012. Phosphatidylinositol 4-kinases: hostages harnessed to build panviral replication platforms. Trends Biochem. Sci. 37, 293–302. https://doi.org/10.1016/j.tibs.2012.03.004.

Audhya, A., Emr, S.D., 2002. Stt4 PI 4-kinase localizes to the plasma membrane and functions in the Pkc1-mediated MAP kinase cascade. Dev. Cell 2, 593–605.

Baird, D., Stefan, C., Audhya, A., Weys, S., Emr, S.D., 2008. Assembly of the PtdIns 4-kinase Stt4 complex at the plasma membrane requires Ypp1 and Efr3. J. Cell Biol. 183, 1061–1074. https://doi.org/10.1083/jcb.200804003.

Balakrishnan, S.S., Basu, U., Raghu, P., 2015. Phosphoinositide signalling in Drosophila. Biochim. Biophys. Acta Mol. Cell Biol. Lipids 1851, 770–784. https://doi.org/10.1016/j.bbalip.2014.10.010.

Balakrishnan, S.S., Basu, U., Shinde, D., Thakur, R., Jaiswal, M., Raghu, P., 2018. Regulation of PI4P levels by PI4KIIIα during G-protein-coupled PLC signaling in *Drosophila* photoreceptors. J. Cell Sci. 131, jcs217257 https://doi.org/10.1242/jcs.217257.

Balla, T., 2013. Phosphoinositides: tiny lipids with giant impact on cell regulation. Physiol. Rev. 93, 1019–1137. https://doi.org/10.1152/physrev.00028.2012.

Baskin, J.M., Wu, X., Christiano, R., Oh, M.S., Schauder, C.M., Gazzerro, E., Messa, M., Baldassari, S., Assereto, S., Biancheri, R., Zara, F., Minetti, C., Raimondi, A., Simons, M., Walther, T.C., Reinisch, K.M., De Camilli, P., 2016. The leukodystrophy protein FAM126A (hyccin) regulates PtdIns(4)P synthesis at the plasma membrane. Nat. Cell Biol. 18, 132–138. https://doi.org/10.1038/ncb3271.

Brill, J.A., Hime, G.R., Scharer-Schuksz, M., Fuller, M.T., 2000. A phospholipid kinase regulates actin organization and intercellular bridge formation during germline cytokinesis. Development 127, 3855–3864.

Briscoe, J., Thérond, P.P., 2013. The mechanisms of Hedgehog signalling and its roles in development and disease. Nat. Rev. Mol. Cell Biol. 14, 416–429. https://doi.org/10.1038/nrm3598.

Chakrabarti, P., Kolay, S., Yadav, S., Kumari, K., Nair, A., Trivedi, D., Raghu, P., 2015. A dPIP5K dependent pool of phosphatidylinositol 4,5 bisphosphate (PIP2) is required

for G-protein coupled signal transduction in Drosophila photoreceptors. PLoS Genet. 11, e1004948 https://doi.org/10.1371/journal.pgen.1004948.
Chung, J., Nakatsu, F., Baskin, J.M., De Camilli, P., 2015. Plasticity of PI4KIIIα interactions at the plasma membrane. EMBO Rep. 16, 312–320. https://doi.org/10.15252/embr.201439151.
Dekanty, A., Milán, M., 2011. The interplay between morphogens and tissue growth. EMBO Rep. 12, 1003–1010. https://doi.org/10.1038/embor.2011.172.
Forbes, A.J., Nakano, Y., Taylor, A.M., Ingham, P.W., 1993. Genetic analysis of hedgehog signalling in the Drosophila embryo. Dev. Suppl. 115–124.
Giansanti, M.G., Belloni, G., Gatti, M., 2007. Rab11 is required for membrane trafficking and actomyosin ring constriction in meiotic cytokinesis of Drosophila males. Mol. Biol. Cell 18, 3250–3263. https://doi.org/10.1091/mbc.E07.
Gupta, A., Fabian, L., Brill, J.A., 2018. Phosphatidylinositol 4,5-bisphosphate regulates cilium transition zone maturation in Drosophila melanogaster. J. Cell Sci. 131, jcs218297 https://doi.org/10.1242/jcs.218297.
Gupta, A.R., Pirruccello, M., Cheng, F., Kang, H.J., Fernandez, T.V., Baskin, J.M., Choi, M., Liu, L., Ercan-Sencicek, A.G., Murdoch, J.D., Klei, L., Neale, B.M., Franjic, D., Daly, M.J., Lifton, R.P., De Camilli, P., Zhao, H., Sestan, N., State, M.W., 2014. Rare deleterious mutations of the gene EFR3A in autism spectrum disorders. Mol. Autism. 5, 31. https://doi.org/10.1186/2040-2392-5-31.
Hammond, G.R.V., Fischer, M.J., Anderson, K.E., Holdich, J., Koteci, A., Balla, T., Irvine, R.F., 2012. PI4P and PI(4,5)P2 are essential but independent lipid determinants of membrane identity. Science 337, 727–730. https://doi.org/10.1126/science.1222483.
Hammond, G.R.V., Machner, M.P., Balla, T., 2014. A novel probe for phosphatidylinositol 4-phosphate reveals multiple pools beyond the Golgi. J. Cell Biol. 205, 113–126. https://doi.org/10.1083/jcb.201312072.
Harris, R.E., Setiawan, L., Saul, J., Hariharan, I.K., 2016. Localized epigenetic silencing of a damage-activated WNT enhancer limits regeneration in mature Drosophila imaginal discs. Elife 5, 1–28. https://doi.org/10.7554/eLife.11588.
Hilgemann, D.W., Dai, G., Collins, A., Larricia, V., Magi, S., Deisl, C., Fine, M., 2018. Lipid signaling to membrane proteins: from second messengers to membrane domains and adapter-free endocytosis. J. Gen. Physiol. 150, 211–224. https://doi.org/10.1085/jgp.201711875.
Hille, B., Dickson, E.J., Kruse, M., Vivas, O., Suh, B.-C., 2015. Phosphoinositides regulate ion channels. Biochim. Biophys. Acta Mol. Cell Biol. Lipids 1851, 844–856. https://doi.org/10.1016/j.bbalip.2014.09.010.
Hu, H., Ma, Y., Ye, B., Wang, Q., Yang, T., Lv, J., Shi, J., Wu, H., Xiang, M., 2017. The role of Efr3a in age-related hearing loss. Neuroscience 341, 1–8. https://doi.org/10.1016/j.neuroscience.2016.11.013.
Huang, F.-D.D., Matthies, H.J.G., Speese, S.D., Smith, M.A., Broadie, K., 2004. Rolling blackout, a newly identified PIP_2-DAG pathway lipase required for *Drosophila* phototransduction. Nat. Neurosci. 7, 1070–1078. https://doi.org/10.1038/nn1313.
Jiang, K., Liu, Y., Fan, J., Zhang, J., Li, X.-A., Evers, B.M., Zhu, H., Jia, J., 2016. PI(4)P promotes phosphorylation and conformational change of smoothened through interaction with its C-terminal tail. PLoS Biol. 14, e1002375 https://doi.org/10.1371/journal.pbio.1002375.
Kme, C., Minogue, S., Hsuan, J.J., Waugh, M.G., 2010. Differential effects of the phosphatidylinositol 4-kinases, PI4KIIα and PI4KIIIβ, on Akt activation and apoptosis. Cell Death Dis. 1, 1–8. https://doi.org/10.1038/cddis.2010.84.
Koe, C.T., Tan, Y.S., Lönnfors, M., Hur, S.K., Low, C.S.L., Zhang, Y., Kanchanawong, P., Bankaitis, V.A., Wang, H., 2018. Vibrator and PI4KIIIα govern neuroblast polarity by anchoring non-muscle myosin II. Elife 7 (7), e33555. https://doi.org/10.7554/eLife.33555.
Kolay, S., Basu, U., Raghu, P., 2016. Control of diverse subcellular processes by a single multi-functional lipid phosphatidylinositol 4,5-bisphosphate [PI(4,5)P2]. Biochem. J. 473, 1681–1692. https://doi.org/10.1042/BCJ20160069.
Liu, C.-H., Bollepalli, M.K., Long, S.V., Asteriti, S., Tan, J., Brill, J.A., Hardie, R.C., 2018. Genetic dissection of the phosphoinositide cycle in Drosophila photoreceptors. J. Cell Sci. 131, jcs214478. https://doi.org/10.1242/jcs.214478.
Ma, H., Chitnis, A., Blake, T., Liu, P., Balla, T., 2009. Crucial role of phosphatidylinositol 4-kinase III in development of zebrafish pectoral fin is linked to phosphoinositide 3-kinase and FGF signaling. J. Cell Sci. 122, 4303–4310. https://doi.org/10.1242/jcs.057646.
MacDougall, L.K., Gagou, M.E., Leevers, S.J., Hafen, E., Waterfield, M.D., 2004. Targeted expression of the class II phosphoinositide 3-kinase in Drosophila melanogaster reveals lipid kinase-dependent effects on patterning and interactions with receptor signaling pathways. Mol. Cell Biol. 24, 796–808.
Mandiá, N., Pérez-Muñuzuri, A., López-Suárez, O., López-Sanguos, C., Bautista-Casanovas, A., Couce, M.-L., 2018. Congenital intestinal atresias with multiple episodes of sepsis. Medicine (Baltim.) 97, e10939. https://doi.org/10.1097/MD.0000000000010939.
Martin, T.F.J., 2015. PI(4,5)P2-binding effector proteins for vesicle exocytosis. Biochim. Biophys. Acta Mol. Cell Biol. Lipids 1851, 785–793. https://doi.org/10.1016/j.bbalip.2014.09.017.
Mejillano, M., Yamamoto, M., Rozelle, A.L., Sun, H.Q., Wang, X., Yin, H.L., 2001. Regulation of apoptosis by phosphatidylinositol 4,5-bisphosphate inhibition of caspases, and caspase inactivation of phosphatidylinositol phosphate 5-kinases. J. Biol. Chem. 276, 1865–1872. https://doi.org/10.1074/jbc.M007271200.
Milán, M., Campuzano, S., García-Bellido, A., 1996. Cell cycling and patterned cell proliferation in the wing primordium of Drosophila. Proc. Natl. Acad. Sci. U.S.A. 93, 640–645. https://doi.org/10.1073/pnas.93.2.640.
Nakatsu, F., Baskin, J.M., Chung, J., Tanner, L.B., Shui, G., Lee, S.Y., Pirruccello, M., Hao, M., Ingolia, N.T., Wenk, M.R., De Camilli, P., 2012. PtdIns4P synthesis by PI4KIIIα at the plasma membrane and its impact on plasma membrane identity. J. Cell Biol. 199, 1003–1016. https://doi.org/10.1083/jcb.201206095.
Pagnamenta, A.T., Howard, M.F., Wisniewski, E., Popitsch, N., Knight, S.J.L., Keays, D.A., Quaghebeur, G., Cox, H., Cox, P., Balla, T., Taylor, J.C., Kini, U., 2015. Germline recessive mutations in PI4KA are associated with perisylvian polymicrogyria, cerebellar hypoplasia and arthrogryposis. Hum. Mol. Genet. 24, 3732–3741. https://doi.org/10.1093/hmg/ddv117.
Phan, T.K., Williams, S.A., Bindra, G.K., Lay, F.T., Poon, I.K.H., Hulett, M.D., 2019. Phosphoinositides: multipurpose cellular lipids with emerging roles in cell death. Cell Death Differ. 26, 781–793. https://doi.org/10.1038/s41418-018-0269-2.
Polevoy, G., Wei, H.-C., Wong, R., Szentpetery, Z., Kim, Y.J., Goldbach, P., Steinbach, S.K., Balla, T., Brill, J.A., 2009. Dual roles for the Drosophila PI 4-kinase four wheel drive in localizing Rab11 during cytokinesis. J. Cell Biol. 187, 847–858. https://doi.org/10.1083/jcb.200908107.
Posor, Y., Eichhorn-Grünig, M., Haucke, V., 2015. Phosphoinositides in endocytosis. Biochim. Biophys. Acta Mol. Cell Biol. Lipids 1851, 794–804. https://doi.org/10.1016/j.bbalip.2014.09.014.
Swann, K., Lai, F.A., 2016. The sperm phospholipase C- and Ca2+ signalling at fertilization in mammals. Biochem. Soc. Trans. 44, 267–272. https://doi.org/10.1042/BST20150221.
Tan, J., Brill, J.A., 2014. Cinderella story: PI4P goes from precursor to key signaling molecule. Crit. Rev. Biochem. Mol. Biol. 49, 33–58. https://doi.org/10.3109/10409238.2013.853024.
Tan, J., Oh, K., Burgess, J., Hipfner, D.R., Brill, J.A., 2014. PI4KIIIα is required for cortical integrity and cell polarity during Drosophila oogenesis. J. Cell Sci. 127, 954–966. https://doi.org/10.1242/jcs.129031.
Vervoort, M., Crozatier, M., Valle, D., Vincent, A., 1999. The COE transcription factor Collier is a mediator of short-range Hedgehog-induced patterning of the Drosophila wing. Curr. Biol. 9, 632–639. https://doi.org/10.1016/s0960-9822(99)80285-1.
Von Ohlen, T., Lessing, D., Nusse, R., Hooper, J.E., 1997. Hedgehog signaling regulates transcription through cubitus interruptus, a sequence-specific DNA binding protein. Proc. Natl. Acad. Sci. U.S.A. 94, 2404–2409.
Walch-Solimena, C., Novick, P., 1999. The yeast phosphatidylinositol-4-OH kinase pik1 regulates secretion at the Golgi, 1, 523–525.
Wang, S.L., Hawkins, C.J., Yoo, S.J., Müller, H.A., Hay, B.A., 1999. The Drosophila caspase inhibitor DIAP1 is essential for cell survival and is negatively regulated by HID. Cell 98, 453–463. https://doi.org/10.1016/s0092-8674(00)81974-1.
Wei, H.-C., Sanny, J., Shu, H., Baillie, D.L., Brill, J.A., Price, J.V., Harden, N., 2003. The Sac1 lipid phosphatase regulates cell shape change and the JNK cascade during dorsal closure in Drosophila. Curr. Biol. 13, 1882–1887.
Wong, R., Hadjiyanni, I., Wei, H.-C., Polevoy, G., McBride, R., Sem, K.-P., Brill, J.A., 2005. PIP2 hydrolysis and calcium release are required for cytokinesis in Drosophila spermatocytes. Curr. Biol. 15, 1401–1406. https://doi.org/10.1016/j.cub.2005.06.060.
Yan, Y., Denef, N., Tang, C., Schüpbach, T., 2011. Drosophila PI4KIIIalpha is required in follicle cells for oocyte polarization and Hippo signaling. Development 138, 1697–1703. https://doi.org/10.1242/dev.059279.
Yavari, A., Nagaraj, R., Owusu-Ansah, E., Folick, A., Ngo, K., Hillman, T., Call, G., Rohatgi, R., Scott, M.P., Banerjee, U., 2010. Role of lipid metabolism in smoothened derepression in hedgehog signaling. Dev. Cell 19, 54–65. https://doi.org/10.1016/j.devcel.2010.06.007.